STEM CELLS®

Authored by a member of

IFATS
International Federation for
Adipose Therapeutics and Science

Immunomodulatory Effects of Adipose Stromal Vascular Fraction Cells Promote Alternative Activation Macrophages to Repair Tissue Damage

ANNIE C. BOWLES [ID],[a,b] RACHEL M. WISE,[a] BRITTANY Y. GERSTEIN,[c] ROBERT C. THOMAS,[c] ROBERTO OGELMAN,[c] ISABELLA FEBBO,[c] BRUCE A. BUNNELL[a,d]

Key Words. Adipose stem cells • Stem cell therapy • Neurodegeneration • Immunomodulation • Stromal cells • Th1/Th2 • Alternative activation macrophages

[a]Center for Stem Cell Research and Regenerative Medicine and [d]Department of Pharmacology, Tulane University School of Medicine, New Orleans, Louisiana, USA; [b]Department of Cell and Molecular Biology and [c]Neuroscience Program, Tulane University School of Science and Engineering, New Orleans, Louisiana, USA

Correspondence: Bruce A. Bunnell, Ph.D., Tulane University School of Medicine, 1430 Tulane Avenue, SL-99, New Orleans, Louisiana 70112, USA. Telephone: 504-988-7711; Fax: 504-988-7710; e-mail: bbunnell@tulane.edu

ABSTRACT

The pathogenesis of many diseases is driven by the interactions between helper T (T_H) cells and macrophages. The phenotypes of these cells are functional dichotomies that are persuaded according to the surrounding milieu. In both multiple sclerosis and the experimental autoimmune encephalomyelitis (EAE) model, T_H1 and T_H17 cells propagate autoimmune signaling and inflammation in the peripheral lymphoid tissues. In turn, this proinflammatory repertoire promotes the classical activation, formerly the M1-type, macrophages. Together, these cells infiltrate into the central nervous system (CNS) tissues and generate inflammatory and demyelinating lesions. Our most recent report demonstrated the immunomodulatory and anti-inflammatory effects of adipose stromal vascular fraction (SVF) cells and adipose-derived stem cells (ASCs) that led to functional, immunological, and pathological improvements in the EAE model. Here, a deeper investigation revealed the induction of regulatory T cells and alternative activation, or M2-type, macrophages in the periphery followed by the presence of alternative activation macrophages, reduced cellular infiltrates, and attenuation of neuroinflammation in CNS tissues following intraperitoneal administration of these treatments. Spleens from treated EAE mice revealed diminished T_H1 and T_H17 cell activities and were markedly higher in the levels of anti-inflammatory cytokine interleukin-10. Interestingly, SVF cells were more effective than ASCs at mediating these beneficial changes, which were attributed to their localization to the spleens after administration. Together, SVF cells rapidly and robustly attenuated the propagation of autoimmune signaling in the periphery that provided a permissive milieu in the CNS for repair and possibly regeneration. STEM CELLS 2017;35:2198–2207

SIGNIFICANCE STATEMENT

This study was designed as a deep investigation into the immunomodulatory effects of the uncultured adipose stromal vascular fraction (SVF) cells compared with cultured adipose-derived stem cells (ASCs) as therapy in a model of multiple sclerosis. The collected evidence is a descriptive analysis of the promising effects of the relatively new therapeutic alternative to cultured ASCs, known as the SVF. Our preclinical evidence has a high translational impact for the use of SVF cells as therapy in an autoimmune, neurodegenerative disease milieu. This study demonstrates the efficacy of a leading edge-type therapy and indicates many potential mechanisms that result in clinical, immunological, and pathological improvements during a chronic phase of disease.

INTRODUCTION

Understanding the pathological mechanisms underlying inflammation and autoimmunity are of great importance as these are common features shared by many diseases. When these immune-mediated activities lead to pathology within the central nervous system (CNS), the damage can render a CNS milieu that is insufficient for repair [1, 2]. Multiple sclerosis (MS) is a common autoimmune, neurodegenerative disease that remains an unmet clinical challenge. Although the etiology is unclear, it is accepted that an autoimmune response in the peripheral lymphoid tissues is elicited against myelin, the protein sheath produced by oligodendrocytes that insulates nerve axons in the CNS [2–4]. Autoimmune signaling causes effector T cells and macrophages to be recruited across the blood-brain barrier and infiltrate

into CNS tissues where they generate inflammatory and demyelinating lesions predominantly in areas of white matter [3–8]. Using the widely accepted murine experimental autoimmune encephalomyelitis (EAE) model of MS, many of the immunological and pathological features can be reproduced for preclinical investigations [4, 6, 9].

Our laboratory has reported the therapeutic effects of fresh adipose stromal vascular fraction (SVF) cells and culture-expanded adipose-derived stem cells (ASCs) in the EAE model [10–13]. Recently, we extensively characterized freshly isolated SVF cells and culture-expanded ASCs from murine donors and compared the therapeutic efficacies when administered at late-stage EAE disease. The main subpopulations that comprise the fresh SVF cells were CD34^{+} cells (12.48%), ASCs (9.92%), CD3^{+} T cells (7.57%), adipocytes (6.43%), and macrophages (5.50%). We showed the ability of the SVF cells and ASCs to modulate immune cell activities and improve CNS pathology that partially restored motor function at late-stage disease [11]. With this study, we further demonstrated the cellular mechanisms that mediated these alterations to the phenotypes of helper T (T_H) cell and macrophages in the periphery that attenuated pathology in the CNS. Most importantly, analysis of the spleens and CNS tissue 5 days following treatment with SVF cells or ASCs indicated that both treatments greatly attenuated the activities of T_H1 and T_H17 cells and their associated proinflammatory cytokines. A marked increase in interleukin-10 (IL-10) was correlative to an increased regulatory T cells (Tregs) in the periphery. In turn, this immunomodulation provided a favorable repertoire to induce alternative activation macrophages, previously coined M2, which produced reparative effects in the CNS. Together with our previous reports, SVF cells and ASCs have demonstrated a strong potential for repair and possibly regeneration in the CNS. Moreover, our data demonstrate the use of this easily obtained, uncultured, heterogeneous SVF cells as a therapeutic alternative to culture-expanded ASCs with comparable therapeutic efficacy which has a high impact for many other human indications.

MATERIALS AND METHODS

EAE Induction Using Myelin Oligodendrocyte Glycoprotein$_{35–55}$ Peptide

Reagents for EAE induction were prepared by dilution of myelin oligodendrocyte glycoprotein$_{35–55}$ peptide (MOG; 2 mg/ml; AnaSpec, Fremont, CA, https://www.anaspec.com) in Ultra-Pure distilled water (Invitrogen, Life Technologies, Grand Island, NY, https://www.thermofisher.com) emulsified with equal parts of complete Freund's adjuvant (BD Biosciences Franklin Lakes, NJ, https://www.bdbiosciences.com) containing 8 mg/ml *Mycobacterium tuberculosis* H37RA (#231131; BD Biosciences). MOG emulsion was transferred to 1 ml Luer-Lok syringes (BD Falcon) with 27G 1/2 inch needles. Pertussis toxin was diluted in UltraPure (2 ng/μl; List Biologicals Laboratories, Campbell, CA, https://www.listlabs.com) and transferred to syringes as described above. While anesthetized under 5% isoflurane gas, 6-8 week old female C57Bl/6 mice (Charles River Laboratories, Wilmington, MA, http://www.crivers.com) were induced with EAE by subcutaneous injection of 100 μl MOG emulsion near flanking regions of the tail (200 μl total per

mouse). Mice were concomitantly administered 100 μl pertussis toxin via intraperitoneal (i.p.) injection. After 48 hours, mice received a second i.p. injection of 100 μl pertussis toxin to complete the induction procedure. Mice designated in the sham control group received equivalent volumes and injections containing only Hank's balanced salt solution (HBSS; Gibco; Thermo Fisher Scientific, Waltham, MA, https://www.thermofisher.com). All animal procedures were approved by the Institutional Animal Care and Use Committee at Tulane University and were in compliance with state and federal National Institute of Health's animal welfare regulations. Mice were given food pellets and water *ad libitum*.

Isolation of the SVF Cells and ASCs. Inguinal white adipose tissue was collected from enhanced green fluorescence protein (eGFP) transgenic female mice (C57Bl/6-Tg(UBC-GFP)30Scha/J strain; Jackson Laboratory, Bar Harbor, ME, https://www.jax.org) between the ages of 6–12 weeks. Adipose was washed 3–4 times with phosphate-buffered saline (PBS; Hyclone Laboratories, Inc., Logan, UT, http://www.gelifesciences.com) and finely minced. Adipose was then transferred to a digestion solution containing 0.1% (w/v) collagenase type I (Sigma-Aldrich, St. Louis, MO, https://www.sigmaaldrich.com) and 1% (w/v) bovine serum albumin (BSA; Sigma-Aldrich) in PBS and placed in an incubator shaker set to 100 rpm at 37°C for 1 hour. Digestion reaction was neutralized with complete culture media (CCM) that contained Dulbecco's Modified Eagle Medium: Nutrient Mixture F-12 (Life Technologies), 10% fetal bovine serum (Atlanta Biologicals, Inc., Flowery Branch, GA, https://www.atlanta-biologicals.com), 100 units/ml antimycotic/antibiotic (Life Technologies), and 2 mM L-glutamine (Life Technologies). Digested tissue was filtered through a sterile gauze and centrifuged to obtain the pellet of SVF cells.

For the isolation of ASCs, SVF cells were plated in 15 cm culture dishes containing CCM, which was incubated at 37°C with 5% humidified CO_2. After 24 hours, plates were washed of non-adherent cells with PBS, and fresh CCM was added to each plate. When 70% confluence was achieved, cells were passaged by trypsinization with 0.25% trypsin/1 mM EDTA (Gibco), neutralized with v/v CCM, centrifuged, and re-seeded onto culture dishes at a density of 100–200 cells per square centimeter. This process was repeated for subsequent passages then cells were cryopreserved before experimental use.

Preparation and Injection of Cells

Based on past EAE studies, the day for late-stage therapeutic administration was designated as 20 days post induction (DPI) when motor impairment is greatest and lesions are disseminated throughout the CNS. At 20 DPI, PBS was used to wash freshly isolated SVF cells and cryopreserved ASCs (passage 3–4) before injection. Cells were counted using a trypan blue exclusion method on a hemocytometer. Subsequently, ASCs and SVF cells were re-suspended in HBSS at concentrations of 10^7 cells/ml and transferred to 1 ml Leur-Lok syringes with 27G 1/2 inch needles. EAE mice were randomly designated to treatment groups: ASC treatment, SVF treatment, or vehicle control groups, and received an i.p. injection of 100 μl containing 10^6 ASCs, 10^6 SVF cells, or HBSS, respectively.

Tissue Harvest and Processing

At 5 days (25 DPI) and 10 days (30 DPI) after treatment, EAE mice were sacrificed by CO_2 asphyxiation and blood was immediately collected by intracardial puncture. Following, mice were perfused with sterile PBS, and the spleens and CNS tissues of each EAE mouse were harvested. The blood was allowed to clot at room temperature (RT) for 30 minutes, centrifuged, and then the sera was transferred to tubes and stored at $-80°C$ until further use. Cervical sections of spinal cords were removed and stored at RT in formalin for paraffin-embedding. Remaining CNS tissues were mechanically digested using a 15-ml Dounce homogenizer. The homogenates were then passed through a cell strainer into a 50-ml conical tube and centrifuged at 2000 rpm for 5 minutes. Ficoll-Paque Premium (GE Healthcare Bio-Sciences, Pittsburgh, PA, http://www.gelifesciences.com) was prepared fresh as the 100% isotonic solution by diluting nine parts Ficoll-Paque Premium with one part 10X PBS. Additional isotonic solutions (40% and 70%) were prepared by dilution with HBSS. Cell pellets were obtained and re-suspended in 40% isotonic solution that was carefully overlayed on top of 70% isotonic solution in a conical tube. The samples were centrifuged for 30 minutes at 2000 rpm at $18°C$ without the brake. Mononuclear cells from CNS tissues were collected from the 40%/70% interface, washed with PBS, and counted. Samples were then processed for flow cytometric analysis or stored at $-80°C$ for RNA isolation.

Harvested spleens were mechanically digested through cell strainers using the blunt ends of syringes. The cells were then incubated with red blood cell lysis for 5 minutes at RT. Following, the splenocytes were washed with PBS and counted. Splenocytes were then processed for flow cytometric analysis or stored at $-80°C$ for RNA isolation.

Flow Cytometric Staining and Analysis. CNS cells and splenocytes were counted using a hemocytometer and prepared in staining buffer containing 1% BSA and 1% CD16/CD32 Mouse BD Fc Block (BD Biosciences). Next, cells were stained with fluorescently conjugated anti-mouse antibodies against CD3, CD4, CD45, CD11b, CD11c, CD86, and CD206 (eBioscience). Designated samples were incubated in a fixation/permeabilization solution (eBioscience), stained with a fluorescently conjugated anti-mouse antibody against intracellular foxp3, washed, and stored in buffer solution. All other samples were fixed using 1% paraformaldehyde, washed and stored in buffer solution. The samples were stored at $4°C$ until further analysis.

Flow cytometric analysis of each sample was performed using a BD LSRFortessa (BD Biosciences) instrument. Data analysis was acquired of 10,000 events using FlowJo software (FlowJo, LLC, Ashland, OR, http://www.flowjo.com) for representative samples in each group ($n = 4$).

RNA Isolation from CNS Tissue and Spleens. Briefly, Qiazol Tissue Protectant (Qiagen, Valencia, CA, http://www.qiagen.com) was added to cells isolated from the CNS tissues and spleens. Total RNA extraction was performed for each sample using the RNeasy Mini Kit (Qiagen) according to the manufacturer's instructions. RNA was subsequently purified with DNase I (Invitrogen) and 1 μg RNA was reverse transcribed using the SuperScript VILO cDNA synthesis kit (Invitrogen). EXPRESS SYBR GreenER qPCR SuperMix Kit (Invitrogen) was used for quantitative reverse transcriptase polymerase chain reaction (qPCR) using mouse-specific primers to IL-2 receptor forward 5′-GGCTCTTCTTGGAGATGCTG-3′, reverse 5′-GCCAGAAAAACAAC CAAGGA-3′, IL-4 forward 5′-GGTCTCAACCCCCAGCTAGT-3′, reverse 5′-GCCGATGATCTCTCTCAAGTGAT-3′, IL-23A forward 5′-CAAAGGATCCGCCAAGGTCT-3′, reverse 5′- GGAGGTGTGAAGTT GCTCCA-3′, and eGFP forward 5′- GGGCACAAGCTGGAGTA CAAC-3′, reverse 5′-CACCTTGATGCCGTTCTTCTG-3′. All other primer sequences were previously reported [11]. For GFP detection, qPCR data were calculated and reported as the log ($-\Delta Ct$) to represent the levels of GFP mRNA. All other qPCR data were calculated and reported as the $\Delta\Delta Ct$ values that were normalized to the vehicle control group for quantitative comparison of mRNA expression levels. Values were represented as the mean $\pm$ SEM of the relative fold change for each group ($n = 3$).

Histological Analysis of Spinal Cords. Formalin fixed cervical spinal cords were paraffin-embedded, cut 5 microns thick, and mounted on microscope slides. Sections were stained with H&E (Richard-Allan Scientific, Thermo Fisher Scientific) and scanned into Imagescope software (Aperio Technologies, Inc., Vista, CA, http://www.leicabiosystems.com) using an Aperio Scanscope CS2 instrument (Aperio Technologies, Inc.). For each section, three images of randomly selected fields of white matter were taken at 40X magnification. Each image was then uploaded onto Fiji/Image J software (National Institutes of Health, Bethesda, MD, https://imagej.nih.gov) and cells were counted according to the number of pixels and circularity. For each mouse section, 3 fields were measured for cellular infiltrates per group ($n = 5$).

Additional sections were used for immunohistochemical analysis. Briefly, sections were de-paraffinized, rehydrated, and heat-mediated antigen retrieval was performed. Sections incubated with blocking solution containing: 10% goat serum, and 1% BSA in Tris buffered solution (TBS), for 1 hour at RT. Designated sections were then stained with primary antibody rat anti-mouse glial fibrillary acidic protein (GFAP; 1:200, Life Technologies) followed by secondary goat anti-rat IgG Alexa Fluor 594 (Invitrogen Molecular Probes, Eugene, OR, http://www.thermofisher.com/invitrogen). Rat anti-mouse primary antibodies F4/80 (Invitrogen) and goat anti-mouse Arginase-1 (Arg-1; 1:200, Santa Cruz Biotechnology, Dallas, TX, https://www.scbt.com) were prepared in staining buffer containing 1% BSA in TBS and incubated on spinal cord sections overnight at $4°C$. Sections were then washed and incubated with secondary antibodies: goat anti-rat IgG Alexa Fluor 488 (Invitrogen Molecular Probes) and donkey anti-goat IgG Alexa Fluor 647 (Abcam, Cambridge, MA, http://www.abcam.com) for 1 hour at RT. Additional washes were then followed by mounting with ProLong Gold anti-fade reagent with DAPI (Life Technologies) and a coverslip. Images were taken at 40X magnification along the perivascular regions of the spinal cords using a Nikon Eclipse E800 (Nikon, Melville, NY, http://www.nikon.com) microscope with Slidebook version 5.0 software (Olympus, Center Valley, PA, http://www.olympusmicro.com).

Detection of Serum Proteins Using an Enzyme-Linked Immunosorbent Assay. Sera stored at $-80°C$ were thawed and equal amounts were pooled together to represent samples for each group ($n = 7$). Samples were added to the wells of an ELISArray plate of the Mouse Th1/Th2/Th17 Cytokines
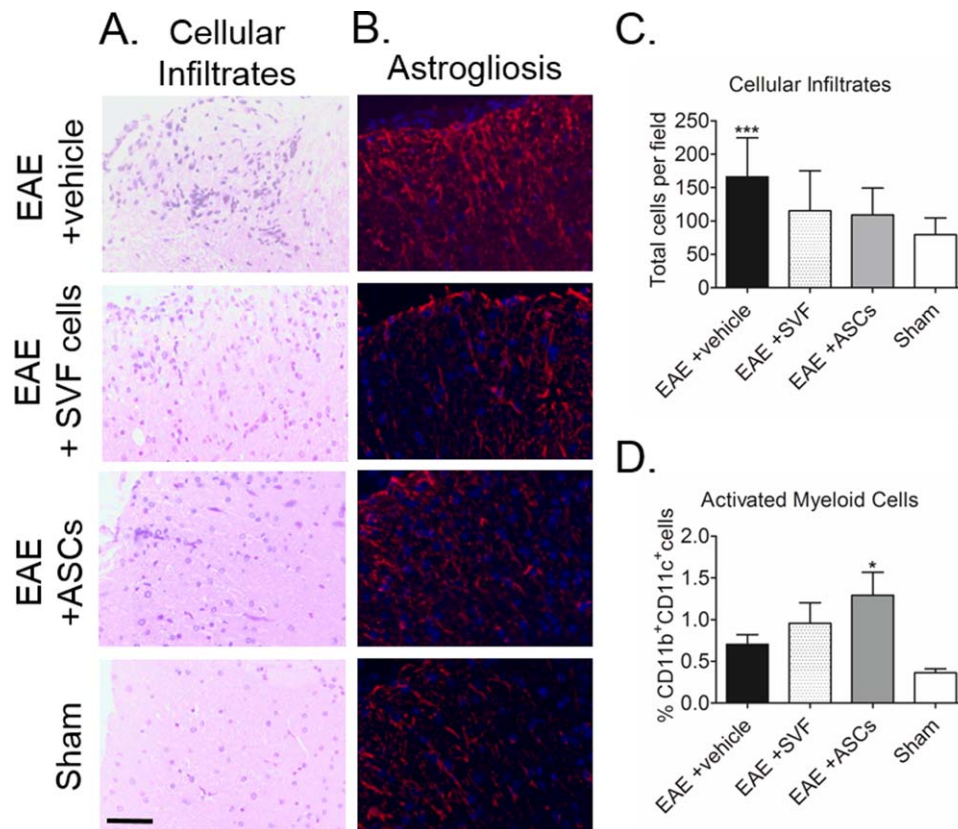
Figure 1. Histopathology of central nervous system (CNS) showed improvements 5 days following treatment with stromal vascular fraction (SVF) cells and adipose-derived stem cells (ASCs). **(A):** The levels of the cellular infiltrates present in the spinal cords of mice in each group were displayed in representative images. **(B):** Glial fibrillary acidic protein expressed on astrocytes demonstrated the degree of astrogliosis associated with neuroinflammation which was visualized in spinal cord sections for each group. **(C):** Quantitative analysis demonstrated a significant reduction in cellular infiltrates following treatment with SVF cells and ASCs. **(D):** Detection of $CD11b^+CD11c^+$ cells determined the increased frequency of activated microglia within the CNS of EAE mice treated with SVF cells and more so ASCs. Scale bars = 50 μm. *, $p < .05$; **, $p < .01$; ***, $p < .001$ compared with sham-treated EAE group. Abbreviations: ASC, adipose-derived stem cell; EAE, experimental autoimmune encephalomyelitis; SVF, stromal vascular fraction.

Multi-Analyte ELISArray Kit (MEM-003A; SABiosciences, Qiagen) and processed according to the manufacturer's protocol. The plate was read at absorbance (450 nm) and values were corrected by subtraction of the negative control values.

Statistical Analysis

All values reported for the SVF-, ASC-, and vehicle-treated EAE mice were quantitatively compared with the sham control group. Statistical analyses were performed using one-way analysis of variance followed by pairwise comparisons of the mouse groups using Bonferroni *post hoc* testing. Significance for the overall group effect and individual pairwise comparisons were made against the sham-treated EAE group and defined as $p < .05$. Analysis was performed using Prism 5.0 (Graphpad Software, La Jolla, CA, https://www.graphpad.com).

RESULTS

SVF Cells and ASCs Reduce the Levels of Cellular Infiltrates in the Spinal Cords

Cervical spinal cord sections were stained with H&E to visualize the presence of cells within the white matter (Fig. 1A). Quantitative comparison with sham controls (79.5 ± 25.02 cells)

determined significantly higher levels of infiltrates higher levels of cellular infiltration in the vehicle treated EAE group (166.2 ± 58.4 cells; $p < .001$) and improvements to the levels of infiltrates 5 days following injection of SVF cells (115.3 ± 59.8 cells) and ASCs (109.3 ± 39.9 cells; Fig. 1C). Representative images of spinal cord sections stained with GFAP demonstrated the level of astrogliosis associated with neuroinflammation among all groups. Reduced GFAP staining suggested that after 5 days of treatment with SVF cells and ASCs, attenuation of neuroinflammation occurred (Fig. 1B). The frequency of activated myeloid cells defined by the expression of $CD11b^+CD11c^+$ cells in the CNS tissues was measured using flow cytometric analysis. The frequency of activated myeloid cells following treatment with SVF cells (0.96 ± 0.25%) was comparable with the vehicle-treated EAE group (0.71 ± 0.12%) and sham controls (0.36 ± 0.05%). Contrastingly, treatment with ASCs (1.29 ± 0.27%; $p < .05$) enhanced the frequency of activated myeloid cells in the CNS tissues (Fig. 1D).

Alternative Activation Macrophage Phenotype was Detected in Perivascular Locations of the CNS Following Treatment with SVF Cells and ASCs. The presence of the alternative activation macrophage phenotypes was detected by co-expression of $F4/80^+Arg-1^+$ in the spinal cord sections of
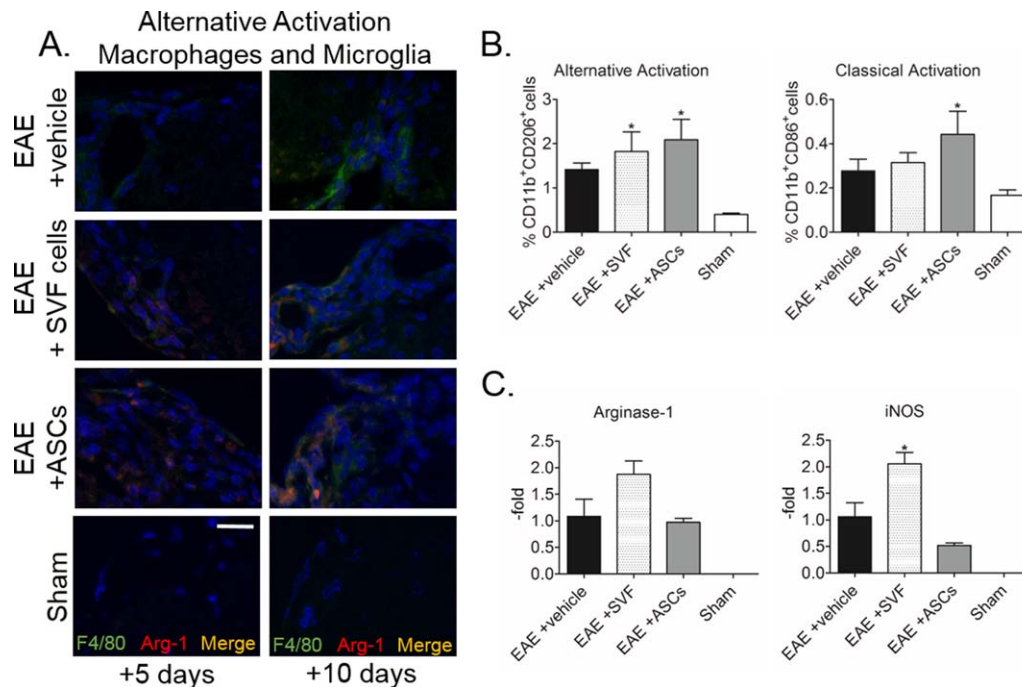
Figure 2. Stromal vascular fraction (SVF) cells and adipose-derived stem cells (ASCs) promoted an alternative activation phenotype of macrophages in central nervous system (CNS) tissues. **(A):** Co-expression of F4/80 and arginase-1 (Arg-1) demonstrated the presence of the alternative activation macrophage phenotype in the perivascular locations of the spinal cords shown 5 and 10 days following treatment with SVF cells and ASCs. **(B):** The frequency of alternative and classical activation macrophage phenotypes was determined by detection of $CD11b^+CD206^+$ and $CD11b^+CD86^+$ cells, respectively, in the CNS 5 days following treatment. **(C):** Gene expression levels of Arg-1 and induced nitric oxide synthase measured in the CNS tissues of mice in each group showed SVF treatment induced the largest changes to macrophage phenotypes 10 days after treatment. Scale bars = 50 μm. *, $p < .05$; **, $p < .01$; ***, $p < .001$ compared with sham-treated EAE group. Abbreviations: ASC, adipose-derived stem cell; EAE, experimental autoimmune encephalomyelitis; SVF, stromal vascular fraction.

mice in each group. Representative images showed alternative activation macrophages within the perivascular areas adjacent to lesions at both 5 and 10 days after treatment with both SVF cells and ASCs, but not in the vehicle-treated EAE or sham control groups (Fig. 2A). Flow cytometric analysis of CNS tissues demonstrated the frequencies of both the alternative and classical activation phenotypes of macrophages by the detections of $F4/80^+CD206^+$ cells and $F4/80^+CD86^+$ cells, respectively, in the CNS tissues from mice in each group. Alternative activation macrophages were detected at higher frequencies 5 days after treatment in the SVF-treated (1.82% ± 0.45%; $p < .05$) and ASC-treated (2.09% ± 0.46%; $p < .05$) EAE mice compared with the vehicle-treated EAE mice (1.42% ± 0.15%) and sham controls (0.40% ± 0.03%). In contrast, the levels of the classical activation phenotype of macrophages 5 days following SVF treatment (0.32% ± 0.44%) were comparable with the vehicle-treated (0.28% ± 0.53%) and sham control (0.17% ± 0.02%) EAE mice, while an increase was detected 5 days following treatment with ASCs (0.44% ± 0.10%; $p < .05$; Fig. 2B). Gene expression levels of enzymes Arg-1 and induced nitric oxide synthase (iNOS) associated with the polarization of phenotype to either the alternative or classical activation macrophage, respectively, were indicated in the CNS 10 days following treatment. Quantitative comparison showed treatment with SVF cells induced 1.88 ± 0.25-fold higher expression of Arg-1 compared with treatment with vehicle (1.09 ± 0.33-fold) and ASCs (0.97 ± 0.08-fold). Likewise, treatment with SVF cells enhanced iNOS expression to 2.06 ± 0.21-fold ($p < .05$) higher

than treatment with vehicle (1.05 ± 0.27-fold) while iNOS treatment was 0.52 ± 0.04-fold less following treatment with ASCs. The expressions of Arg-1 and iNOS were undetectable in the CNS tissues of sham control group (Fig. 2C).

Splenic Myeloid and Lymphoid Cell Populations Reveal the Largest Differences Following SVF Treatment. Based on $CD45^+$ expression, comparisons of total splenocytes 5 days following treatment showed comparable frequencies amongst the vehicle- (91.20% ± 2.32%), SVF-(97.01% ± 1.06%), ASC-(96.29% ± 1.48%) treated, and sham control (93.35% ± 2.72%) groups. However, co-expression with $CD11b^+$ defined cells of the myeloid cell lineages. Compared with the sham control group (11.42% ± 1.70%), the splenic myeloid cells of the EAE induced mice were all markedly increased at 25 DPI. More specifically, the myeloid cells of the EAE mice treated with vehicle were 33.83% ± 8.78% ($p < .05$), and treatment with SVF (48.16% ± 1.78%; $p < .001$), and ASCs (42.52% ± 1.35%; $p < .01$) further enhanced the frequencies of these populations in the spleens after 5 days (Fig. 3A).

T_H cells were identified in the spleen by the $CD3^+CD4^+$ phenotypic expression, and Tregs were further defined as $CD3^+CD4^+CD25^+foxp3^+$ phenotypic cells. Unlike the splenic myeloid cell populations, the detected T lymphocyte populations of the sham controls were higher than those amongst the EAE induced mice. Compared with the frequency of T_H cells in the sham control group (21.83% ± 1.05%), the frequencies of T_H cells in EAE mice treated with vehicle (9.60% ± 1.51%; $p < .001$) and ASCs (9.36% ± 0.39%; $p < .001$) were
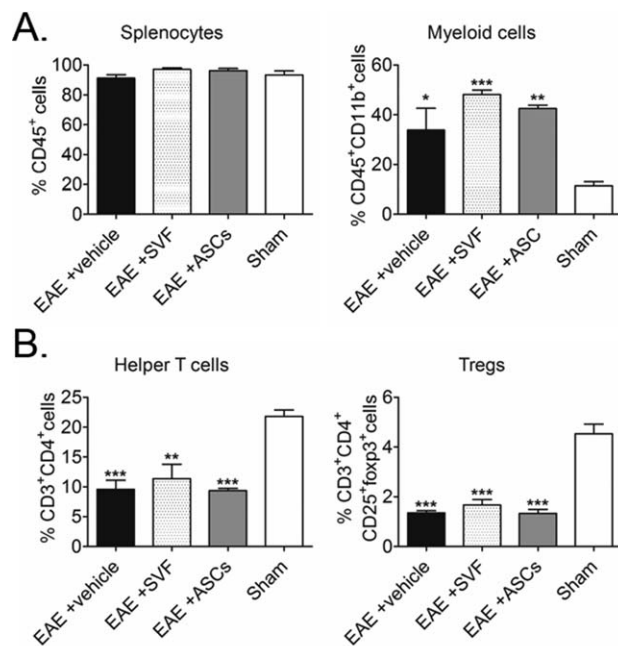
Figure 3. Frequencies of cells within the spleens of treated experimental autoimmune encephalomyelitis mice revealed modest increases in myeloid and lymphoid populations 5 days after treatment. **(A):** Leukocytes were detected and measured by expression of CD45$^+$ within the spleen of mice in each group. Leukocytes were further defined as myeloid cells by the co-expression with CD11b$^+$. **(B):** The frequencies of helper T cells and regulatory T cells were modestly altered 5 days after treatment with stromal vascular fraction cells and adipose-derived stem cells. This data validated the myeloid and non-myeloid of the previous panel of the splenocyte expressions of each mice per group. *, $p < .05$; **, $p < .01$; ***, $p < .001$ compared with sham-treated EAE group. Abbreviations: ASC, adipose-derived stem cell; EAE, experimental autoimmune encephalomyelitis; SVF, stromal vascular fraction.

most significantly and comparably reduced 5 days following administration of treatment. Similarly, but to a lesser extent, the frequencies of T_H cells within the spleen 5 days following SVF treatment were marked reduced (11.39% $\pm$ 2.41%; $p < .01$) compared with the sham controls.

At 25 DPI, the frequency of splenic Treg populations of the sham controls was 4.54% $\pm$ 0.38%. By comparison, the frequencies of Tregs in all EAE groups were significantly reduced 5 days following treatment. Amongst the EAE groups, the Tregs within the spleens of SVF-treated mice (1.67% $\pm$ 0.22%; $p < .001$) were highest compared with the vehicle- (1.35% $\pm$ 0.09%; $p < .001$) and ASC-treated (1.33% $\pm$ 0.16%; $p < .001$) mice, respectively (Fig. 3B).

Alternative Activation Macrophages Were Rapidly Induced in the Spleens Following SVF Treatment. The expression levels of Arg-1, which are associated with the alternative activation macrophages, were measure 5 and 10 days after treatment. The highest levels of Arg-1 were measured in splenocytes 5 days after treatment with SVF cells (3.56 $\pm$ 1.01-fold; $p < .05$) compared with those in EAE mice treated with vehicle (1.02 $\pm$ 0.16-fold) and ASCs (1.70 $\pm$ 0.09-fold) or sham controls (0.34 $\pm$ 0.14-fold). At 10 days after treatment, levels of Arg-1 were highest in the spleens of EAE mice treated with ASCs (2.73 $\pm$ 1.6-fold), followed by treatment with SVF cells

(1.52 $\pm$ 0.34-fold), vehicle (1.10 $\pm$ 0.36-fold), and sham controls (0.10 $\pm$ 0.04-fold; Fig. 4A). The expressions of iNOS in the spleens were highly variable for all mice in each group and consequentially unable to achieve statistical comparisons (data not shown).

SVF Cells and ASCs were Detected in the Spleens 5 Days Following Treatment. Cells used as treatment in this study were isolated from GFP-expressing transgenic mice and then administered to EAE mice via i.p. injection. After 5 days, GFP-expression was analyzed within harvested spleens to determine whether injected cells were still present. Evidence determined that ASCs (6.01 $\pm$ 0.88 $\times$ 10^4) and an even markedly higher presence of GFP was detected in the EAE group treated with SVF cells (2.26 $\pm$ 0.40 $\times$ 10^3; $p < .001$). The levels of GFP were undetectable in the vehicle-treated EAE group and sham controls (Fig. 4B).

SVF Cells and Not ASCs Promoted the Expansion of T Cells Suggesting Autologous Use for Translational Applications. To determine the propagation of T cell signaling and proliferation responses to treatments, the IL-2 receptor (IL-2R) was measured. The gene expression levels of IL-2R was highest following treatment with SVF cells (1.41 $\pm$ 0.18-fold) compared with the vehicle (1.01 $\pm$ 0.10-fold) and ASC (0.99 $\pm$ 0.16-fold) treatment groups and sham controls (0.96 $\pm$ 0.13-fold; Fig. 4C).

Gene Expression Cytokine Profile of Spleens Following Treatment with SVF Cells and ASCs Show Promotion of Tregs and Suppression of T_H1 and T_H17 Cells. The expression levels of cytokines relevant to specific T_H cell subsets were quantitatively compared in splenocytes 5 days after treatment. For cytokines associated with Tregs, the levels of IL-10 and transforming growth factor (TGF)-β were measured. For IL-10 levels, splenocytes from SVF-treated EAE mice (20.72 $\pm$ 6.76-fold; $p < .05$) were markedly higher than from those measured in the vehicle- (1.17 $\pm$ 0.61-fold) and ASC-treated (9.94 $\pm$ 1.26-fold) EAE mice and sham controls (0.25 $\pm$ 0.08-fold). Comparable levels of TGF-β were seen in the EAE mice treated with vehicle (1.01 $\pm$ 0.10-fold) and SVF cells (1.02 $\pm$ 0.47-fold) while ASC treatment (1.46 $\pm$ 0.34-fold) restored TGF-β levels to those measured in sham controls (1.46 $\pm$ 0.28-fold). Treatment with SVF cells and ASCs reduced the levels IL-4 0.50 $\pm$ 0.18-fold and 0.53 $\pm$ 0.23-fold less, respectively, than vehicle-treated EAE mice (1.09 $\pm$ 0.28-fold) and even less IL-4 measured in the sham controls (0.20 $\pm$ 0.13-fold; Fig. 5).

To determine the presence of T_H1 and T_H17 cells in the spleens 5 days following treatment, the expression levels of interferon-γ (IFNγ), IL-23, IL-12, and IL-17 were analyzed. For the levels of IFNγ, EAE mice treated with SVF cells (0.58 $\pm$ 0.23-fold) and ASCs (0.51 $\pm$ 0.09-fold) and sham controls (0.59 $\pm$ 0.15-fold) were comparably less compared with the vehicle-treated EAE group (1.16 $\pm$ 0.39-fold). The levels of IL-23 were markedly reduced in the sham controls (0.001 $\pm$ 0.0004-fold) and EAE mice following treatment with SVF cells (0.23 $\pm$ 0.05-fold) and ASCs (0.10 $\pm$ 0.04-fold) compared with the vehicle-treated EAE mice (1.13 $\pm$ 0.33-fold; $p < .01$). Similarly, the levels of IL-12 were reduced in the SVF- (0.80 $\pm$ 0.15-fold) and ASC-treated (0.26 $\pm$ 0.09-fold) EAE mice and higher in the vehicle-treated EAE group (1.13 $\pm$ 0.41-fold; $p < .05$) compared with the sham controls
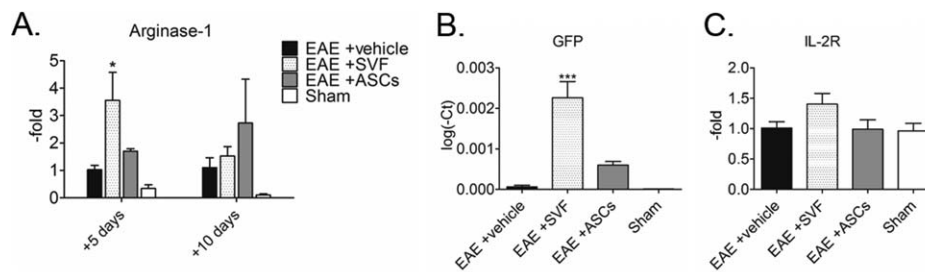
Figure 4. Stromal vascular fraction (SVF) cells localized to the spleen, promoted alternative activation macrophages, and perpetuated T cell signaling. **(A):** Expression of Arginase-1 associated with alternative activation macrophage phenotype was greatly increased 5 days following treatment with SVF cells and 10 days following treatment with adipose-derived stem cells (ASCs). **(B):** Raw cycle analysis of green fluorescence protein detected in the spleens of mice in each group showed ASCs and, more so, SVF cells localize to the spleens 5 days after intraperitoneal injection. **(C):** Interleukin (IL)-2R gene expression levels in the spleens were most enhanced 5 days following SVF compared with all of the other groups. *, $p < .05$; **, $p < .01$; ***, $p < .001$ compared with sham-treated EAE group. Abbreviations: ASC, adipose-derived stem cell; EAE, experimental autoimmune encephalomyelitis; GFP, green fluorescence protein; IL, interleukin; SVF, stromal vascular fraction.
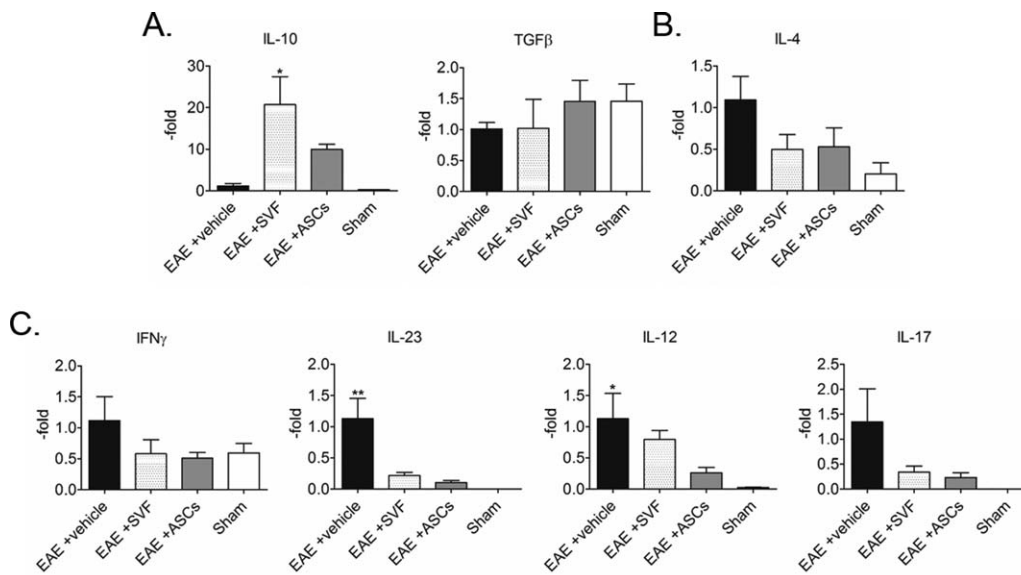

Figure 5. Stromal vascular fraction (SVF) treatment promoted regulatory T cells and suppressed T_H1, T_H2, and T_H17 cells following treatment with SVF cells and adipose-derived stem cells (ASCs). Gene expression levels measured from splenocytes indicated the differentiation of specific helper T cell subsets following treatment. **(A):** Regulatory T cell-associated cytokine expressions were enhanced 5 days after treatment with SVF cells and ASCs. **(B,C):** Contrastingly, the cytokines specific to T_H1, T_H2, and T_H17 cell differentiation were markedly reduced 5 days following treatment with SVF cells and ASCs compared with the vehicle control groups. Physiological comparisons with shams show a cytokine repertoire indicative of non-diseased animals. *, $p < .05$; **, $p < .01$; ***, $p < .001$ compared with sham-treated EAE group. Abbreviations: ASC, adipose-derived stem cell; EAE, experimental autoimmune encephalomyelitis; IFN, interferon; IL, interleukin; SVF, stromal vascular fraction; TGF, transforming growth factor.

(0.03 ± 0.01-fold). The same trend was indicated in the levels of IL-17 measured in the EAE groups following SVF (0.34 ± 0.12-fold) and ASC (0.23 ± 0.10-fold) treatment and undetectable in sham controls compared with the EAE mice treated with vehicle (1.35 ± 0.66-fold; Fig. 5).

Proteins in Circulation Showed Evidence Consistent to the Expression Levels of Cytokines Detected in the Spleens. The protein levels of inflammatory mediators that correspond to T_H cell subsets were detected in the pooled sera of mice 5 days following treatment. Tumor necrosis factor (TNF)-α levels were highest in the vehicle-treated EAE group (0.012 OD) followed by the sham controls (0.09 OD) and ASC-treated EAE group (0.03 OD). The levels of TNF-α were reduced to undetectable levels in the SVF-treated EAE group. Likewise, SVF treatment reduced the levels of IL-17 to undetectable levels compared with the

vehicle- (0.13 OD) and ASC-treated (0.14 OD) and sham controls (0.09). Moreover, the protein levels of IL-23 were lowest in the SVF treatment group (0.05 OD) followed by the vehicle- (0.13 OD) and ASC-treated (0.15 OD) EAE mice and sham controls (0.08 OD). Consistent with the gene expression levels detected in the spleens, the protein levels of TGF-β were highest in the EAE mice treated with SVF cells (0.20 OD) and ASCs (0.18 OD) and sham controls (0.11 OD) compared with the vehicle-treated EAE group (0.001 OD; Fig. 6).

DISCUSSION

In both MS and EAE, effector T cells and macrophages are activated in peripheral lymphoid organs, migrate through the bloodstream, and infiltrate into CNS tissues where they
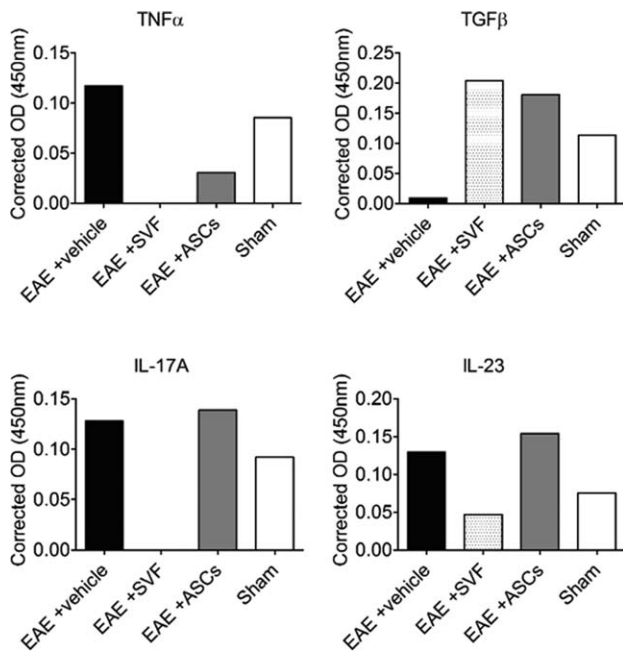
Figure 6. Serum proteins showed diminished inflammatory mediators with stromal vascular fraction and adipose-derived stem cells. After 5 days of treatment, sera was pooled from mice in each group and assessed for inflammatory mediators associated with subsets of helper T cells. The quantity of mediators for each group is represented as a single value of the absorbance measured chemiluminescence. Abbreviations: ASC, adipose-derived stem cell; EAE, experimental autoimmune encephalomyelitis; IL, interleukin; SVF, stromal vascular fraction; TGF, transforming growth factor; TNF, tumor necrosis factor.

generate neuroinflammation and demyelination. These effector T cells are specific subtypes of T_H cells known as the T_H1 and T_H17 that produce inflammatory cytokines including IFNγ, IL-12, IL-23, and IL-17 [14–19]. These inflammatory mediators not only incite neuroinflammation but also direct the differentiation and maintenance of the classical activation macrophage phenotype [20, 21]. During the progression of EAE, macrophages express the classical activation phenotype that additionally release proinflammatory cytokines and damage CNS tissue [21, 22]. Enhancing this proinflammatory phenotype of macrophages showed further aggravation of CNS disease in EAE [22]. Together, this signaling axis between the effector T cells and macrophages are prime targets of immunomodulatory therapies in order to prevent further pathology [23–25].

The functional dichotomy of macrophage phenotypes, termed as the classical activation and the alternative activation phenotypes, is not definitive, but dynamic, and is dependent on the milieu [20, 23]. Much is evidenced about the T_H1 cell-derived IFNγ that directs the classical activation macrophage that functions as proinflammatory [23, 24, 26]. On the contrary, T_H2 cells and Tregs produce IL-4 and IL-10, respectively, which are capable of promoting the alternative activation macrophage phenotype. Increasing evidence has now shown that IL-10 has a more robust effect on inducing alternative activation phenotype of macrophages [27, 28]. Furthermore, many immune cells are capable of expressing IL-10, including Tregs and alternative activation macrophages which, in turn, further increase the levels of IL-10 and promote the differentiation of additional regulatory cells. Together, this
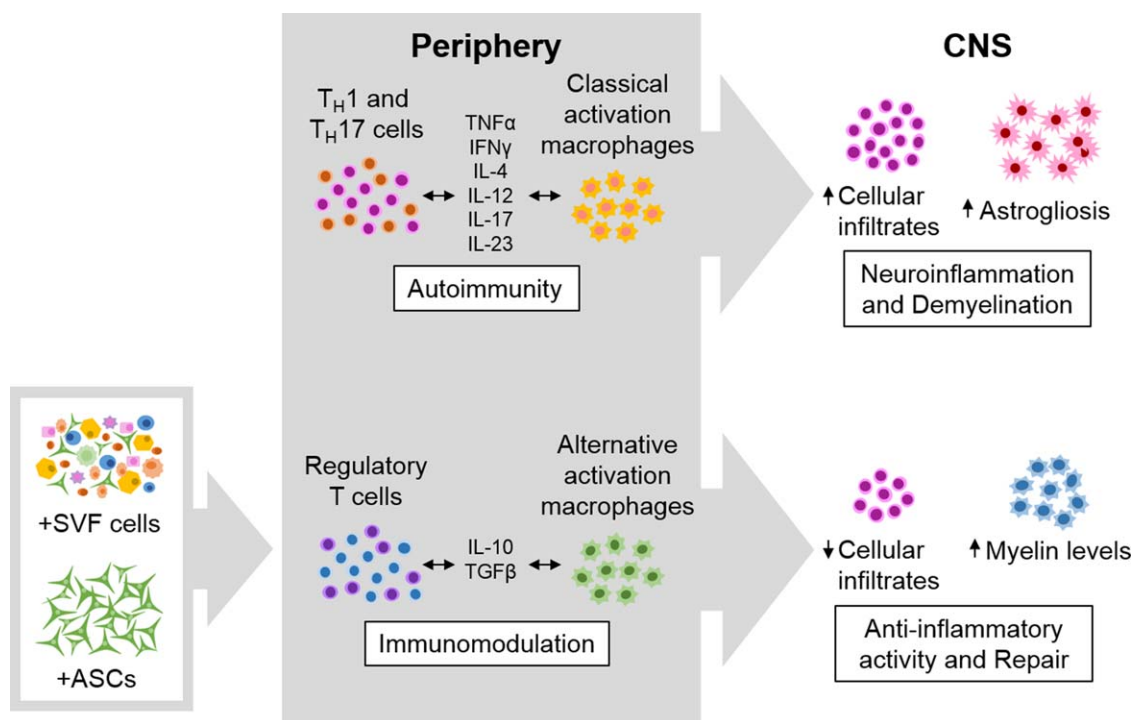

Figure 7. Schematic collectively showing results that lead to improvements in EAE mice following treatment with stromal vascular fraction (SVF) cells and adipose-derived stem cells (ASCs). At late EAE disease stage, treatment with SVF cells and ASCs induced favorable changes in the periphery that then led to amelioration to central nervous system pathology. Abbreviations: ASC, adipose-derived stem cell; CNS, central nervous system; IFN, interferon; IL, interleukin; SVF, stromal vascular fraction; TGF, transforming growth factor; TNF, tumor necrosis factor.

establishes an anti-inflammatory milieu capable of suppressing effector T cell functions [28–30]. Aside from producing IL-10, alternative activation macrophages are critical for promoting reparative and anti-inflammatory effects [24, 28, 31]. Together, many approaches to shift the phenotype of macrophages from classical to alternative activation have been executed that demonstrate substantial improvements in EAE [20, 25, 28, 30].

Our previous study demonstrated comprehensive therapeutic effects of SVF cells and ASCs 10 days after treatment. Induction of Tregs and high levels of IL-10 were measured highest in the peripheral blood and lymphoid tissues following SVF and ASC treatments which was correlative to reduced cellular infiltrates and increased levels of myelin in the CNS. In this study, we analyzed these same tissues 5 days after treatment in order to gain a better understanding that mediated these changes following the treatments. Our data suggest that treatment with ASCs and, more robustly, SVF cells mediated improvements by shifting the T_H cell and macrophage paradigm. This data showed that in multiple tissues cytokines IFNγ, IL-12, IL-23, and IL-17, which are secreted by T_H1 and T_H17 cells, were attenuated following treatment with SVF cells and ASCs. This coincided with a reduction in inflammatory infiltrates and astrogliosis associated with neuroinflammation in CNS tissues.

Moreover, the increased presence of alternative activation macrophages along with high levels of Arg-1 were measured in both the spleens and CNS tissues of EAE mice treated with SVF cells and ASCs. The data suggested that SVF cells promoted a more rapid and robust induction of alternative activation macrophages in the spleens compared with the ASCs. Marked increases in IL-10 and Arg-1 levels were measured in the spleens of EAE mice directly after the administration of SVF cells. Although the expression levels of IL-4 were diminished with SVF and ASC treatments, the analysis 5 days following treatment may not have allowed for detection of T_H2 differentiation. Similarly, at this time, a modest increase in Tregs was observed in the spleens following treatment with SVF cells, and our previous reports showed a more robust induction of Tregs and associated IL-10 at 10 days following treatment.

Growing evidence is suggesting that the dynamic polarization and correlative functions of microglia, the resident macrophages of the CNS, are similar to those of peripheral macrophages [21, 32]. As immune cells of the CNS, microglia can be activated and, depending on the cytokine repertoire, have been shown to either promote propagation of neuroinflammation or play a role in immunosuppression by suppression of T_H17 cells in EAE [21, 32–34]. Together, this evidence correlates the immunomodulatory potency of SVF cells and ASCs in the periphery that are transmitted to the CNS to attenuate neuroinflammation and pathology and mediate repair in EAE (Fig. 7).

CONCLUSION

Currently, fresh SVF cells can be isolated from harvested adipose to supplement fat grafts or used cosmetically during plastic and reconstructive procedures. Adipose can be easily digested, and the SVF cells can be rapidly administered back to patients without the need for laboratories and equipment for culture expansion [35, 36]. Although uncultured SVF cells is proposed as an attractive alternative to culture-expanded ASCs, this heterogeneous composition that contains various leukocytes expressing self-antigens could have detrimental effects. With the translational implications for using fresh SVF cells for therapeutic purposes, it is suggested that autologous administration of SVF cells remains the safest method of use.

AUTHOR CONTRIBUTIONS

A.C.B.: conception and design, provision of study material or patients, collection and/or assembly of data, data analysis and interpretation, manuscript writing; R.M.W., B.Y.G., R.C.T., R.O., and I.F.: collection and/or assembly of data, data analysis and interpretation; B.A.B.: conception and design, financial support, administrative support, provision of study material or patients, manuscript writing, final approval of manuscript.

DISCLOSURE OF POTENTIAL CONFLICTS OF INTEREST

The authors indicated no potential conflicts of interest.

REFERENCES

1 Amor S, Peferoen LA, Vogel DY et al. Inflammation in neurodegenerative diseases. Immunology 2010;129:154–169.

2 Gandhi R, Laroni A, Weiner HL. Role of the innate immune system in the pathogenesis of multiple sclerosis. J Neuroimmunol 2010;221:7–14.

3 Wu GF, Alvarez E. The immunopathophysiology of multiple sclerosis. Neurol Clin 2011;29:257–278.

4 Gold R, Linington C, Lassmann H. Understanding pathogenesis and therapy of multiple sclerosis via animal models: 70 years of merits and culprits in experimental autoimmune encephalomyelitis research. Brain 2006;129:1953–1971.

5 Weiner HL. Multiple sclerosis is an inflammatory T-cell-mediated autoimmune disease. Arch Neurol 2004;61:1613–1615.

6 Fletcher JM, Lalor SJ, Sweeney CM et al. T cells in multiple sclerosis and experimental autoimmune encephalomyelitis. Clin Exp Immunol 2010;162:1–11.

7 Lutz SE, Lengfeld J, Agalliu D. Stem cell-based therapies for multiple sclerosis: Recent advances in animal models and human clinical trials. Regen Med 2014;9:129–132.

8 Lassmann H, Bruck W, Lucchinetti C. Heterogeneity of multiple sclerosis pathogenesis: Implications for diagnosis and therapy. Trends Mol Med 2001;7:115–121.

9 Constantinescu CS, Farooqi N, O'Brien K et al. Experimental autoimmune encephalomyelitis (EAE) as a model for multiple sclerosis (MS). Br J Pharmacol 2011;164:1079–1106.

10 Strong AL, Bowles AC, Wise RM et al. Human adipose stromal/stem cells from obese donors show reduced efficacy in halting disease progression in the experimental autoimmune encephalomyelitis model of multiple sclerosis. STEM CELLS 2016;34:614–626.

11 Bowles AC, Strong AL, Wise RM et al. Adipose stromal vascular fraction-mediated improvements at late-stage disease in a murine model of multiple sclerosis. STEM CELLS 2016;35:532–544.

12 Scruggs BA, Semon JA, Zhang X et al. Age of the donor reduces the ability of human adipose-derived stem cells to alleviate symptoms in the experimental autoimmune encephalomyelitis mouse model. STEM CELLS TRANS MED 2013;2:797–807.

13 Semon JA, Maness C, Zhang X et al. Comparison of human adult stem cells from adipose tissue and bone marrow in the treatment of experimental autoimmune encephalomyelitis. Stem Cell Res Ther 2014;5:2.

14 Cua DJ, Sherlock J, Chen Y et al. Interleukin-23 rather than interleukin-12 is the critical cytokine for autoimmune inflammation of the brain. Nature 2003;421:744–748.

15 Iwakura Y, Ishigame H. The IL-23/IL-17 axis in inflammation. J Clin Invest 2006;116:1218–1222.

16 Leonard JP, Waldburger KE, Goldman SJ. Prevention of experimental autoimmune encephalomyelitis by antibodies against interleukin 12. J Exp Med 1995;181:381–386.

17 Darlington PJ, Touil T, Doucet JS et al. Diminished Th17 (not Th1) responses underlie multiple sclerosis disease abrogation after hematopoietic stem cell transplantation. Ann Neurol 2013;73:341–354.

18 Jager A, Dardalhon V, Sobel RA et al. Th1, Th17, and Th9 effector cells induce experimental autoimmune encephalomyelitis with different pathological phenotypes. J Immunol 2009;183:7169–7177.

19 Zhang GX, Gran B, Yu S et al. Induction of experimental autoimmune encephalomyelitis in IL-12 receptor-beta 2-deficient mice: IL-12 responsiveness is not required in the pathogenesis of inflammatory demyelination in the central nervous system. J Immunol 2003;170:2153–2160.

20 Ding L, Gu H, Gao X et al. Aurora kinase a regulates m1 macrophage polarization and plays a role in experimental autoimmune encephalomyelitis. Inflammation 2015;38:800–811.

21 Jiang Z, Jiang JX, Zhang GX. Macrophages: A double-edged sword in experimental autoimmune encephalomyelitis. Immunol Lett 2014;160:17–22.

22 Hucke S, Eschborn M, Liebmann M et al. Sodium chloride promotes pro-inflammatory macrophage polarization thereby aggravating CNS autoimmunity. J Autoimmun 2016;67:90–101.

23 Martinez FO, Gordon S. The M1 and M2 paradigm of macrophage activation: Time for reassessment. F1000Prime Rep 2014;6:13.

24 Gordon S. Alternative activation of macrophages. Nat Rev Immunol 2003;3:23–35.

25 Mikita J et al. Altered M1/M2 activation patterns of monocytes in severe relapsing experimental rat model of multiple sclerosis. Amelioration of clinical status by M2 activated monocyte administration. Mult Scler 2011;17:2–15.

26 Redente EF, Higgins DM, Dwyer-Nield LD et al. Differential polarization of alveolar macrophages and bone marrow-derived monocytes following chemically and pathogen-induced chronic lung inflammation. J Leukoc Biol 2010;88:159–168.

27 Park-Min KH, Antoniv TT, Ivashkiv LB. Regulation of macrophage phenotype by long-term exposure to IL-10. Immunobiology 2005;210:77–86.

28 Liu C, Li Y, Yu J et al. Targeting the shift from M1 to M2 macrophages in experimental autoimmune encephalomyelitis mice treated with fasudil. PLoS One 2013;8:e54841.

29 Oishi S, Takano R, Tamura S et al. M2 polarization of murine peritoneal macrophages induces regulatory cytokine production and suppresses T-cell proliferation. Immunology 2016;149:320–328.

30 Chen C, Li YH, Zhang Q et al. Fasudil regulates T cell responses through polarization of BV-2 cells in mice experimental autoimmune encephalomyelitis. Acta Pharmacol Sin 2014;35:1428–1438.

31 Saraiva M, O'garra A. The regulation of IL-10 production by immune cells. Nat Rev Immunol 2010;10:170–181.

32 Orihuela R, McPherson CA, Harry GJ. Microglial M1/M2 polarization and metabolic states. Br J Pharmacol 2016;173:649–665.

33 Deshpande P, King IL, Segal BM. Cutting edge: CNS CD11c+ cells from mice with encephalomyelitis polarize Th17 cells and support CD25+CD4+ T cell-mediated immunosuppression, suggesting dual roles in the disease process. J Immunol 2007;178:6695–6699.

34 Murphy AC, Lalor SJ, Lynch MA et al. Infiltration of Th1 and Th17 cells and activation of microglia in the CNS during the course of experimental autoimmune encephalomyelitis. Brain Behav Immun 2010;24:641–651.

35 Zhu M, Zhou Z, Chen Y et al. Supplementation of fat grafts with adipose-derived regenerative cells improves long-term graft retention. Ann Plast Surg 2010;64:222–228.

36 Yoshimura K, Sato K, Aoi N et al. Cell-assisted lipotransfer for facial lipoatrophy: Efficacy of clinical use of adipose-derived stem cells. Dermatol Surg 2008;34:1178–1185.